Supplementary Information

Scalable upcycling of thermoplastic polyolefin into vitrimer through transesterification

G. P. Kar, M. O. Saed and E. M. Terentjev

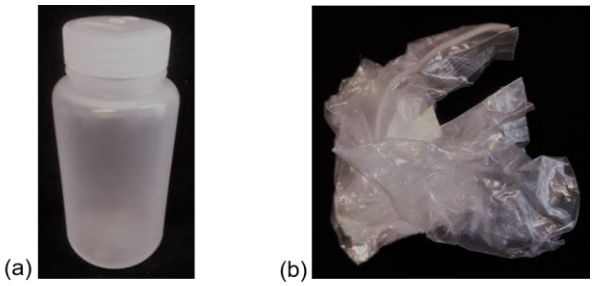

Figure S1. Litter plastics employed as feedstock for the synthesis of polyolefin-vitrimer. a) Recycled bottle made of PP recovered from trash and broken into pieces, b) HDPE packaging that were undergone reactive extrusion.

Table S1. Overview of 'Impact PP' 3950 from Ineos:

MFI	M_w
34 g/10 min	220,400

As formulated by Bremner and Rudin, M_w is calculated as,[1] $\frac{1}{MFI} = GM_w^x$, where the empirical constant $G = 2\times10^{-20}$ (10 min/$g^{(x+1)}$(mol^x)) and $x = 3.40$.

Titration. The efficiency of MA grafting was calculated based on titration method.[2-4] MA moieties on MA-*g*-PP can be hydrolysed with water and that is directly titrated against base (typically alcoholic KOH).[5] Before the titration MA-*g*-PP was kept under vacuum oven at 150 °C for 12 h. 0.5-1.0 g of MA-*g*-PP was dissolved in 50-100 ml of xylene at 120 °C. Few drops of water were added, which makes the solution acidic. 1 wt% bromothymol blue (in dimethyl formamide) was used as indicator: in an acidic solution the indicator appears as yellowish. The acidic solution was then titrated against 0.1 N KOH (in ethanol) until the appearance of faint blue colour is indicating the completion of titration. The amount of KOH (ml) required to reach this point was recorded as a measure of the acidity derived from hydrolysis of MA. The titration was performed in triplicate.

The grafting efficiency of MA was determined by the relation,[5] f = (ml KOH × N × M_m)/ (2 × 10), where the normality, N = 0.1, and M_m = 100 is the molecular weight of grafted MA residue. The resulting percent grafting was obtained as 2.4 wt% (for the 6 wt% of the initial MA added). This grafting efficiency is higher than most cases reported in the literature[2, 6] which we explain by the effect of high-shear mixing in the compounder.

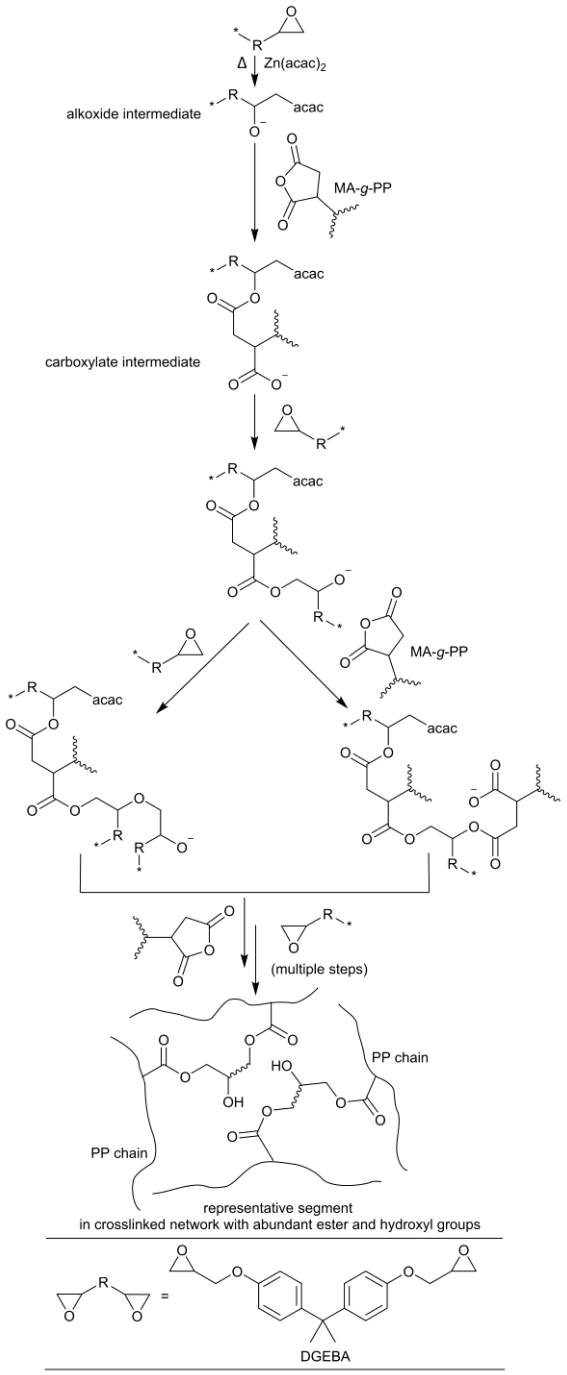

Figure S2. Mechanism of alternating copolymerization of epoxides and anhydride in presence of catalyst $Zn(acac)_2$. The curing process is initiated by the catalyst generating alkoxide intermediates which react anhydride functional groups to produce carboxylate intermediates, that terminate with an -OH group via β-elimination, or again attack epoxy unit generating alkoxides and so on. Thus the alternating copolymerization propagates through (re)generation of alkoxide & carboxylate intermediates.[7-9] Another possible source of proton that form hydroxyl functional groups in the crosslinked network is the water molecule in zinc(II)-acetylacetonate hydrate and DGEBA. As reported by Schlögl et al., at high temperature, water molecule is released from zinc(II)-acetylacetonate hydrate.[10] A similar event occurs with DGEBA, as our procured DGEBA is a viscous liquid with traces of water. Schlögl et al. further reported that with increasing fraction of epoxy (as in our case of the excess DGEBA), they achieved higher -OH content in the crosslinked network that corroborated the increased absorption band at 3482 cm^{-1} in FT-IR spectra.[10]

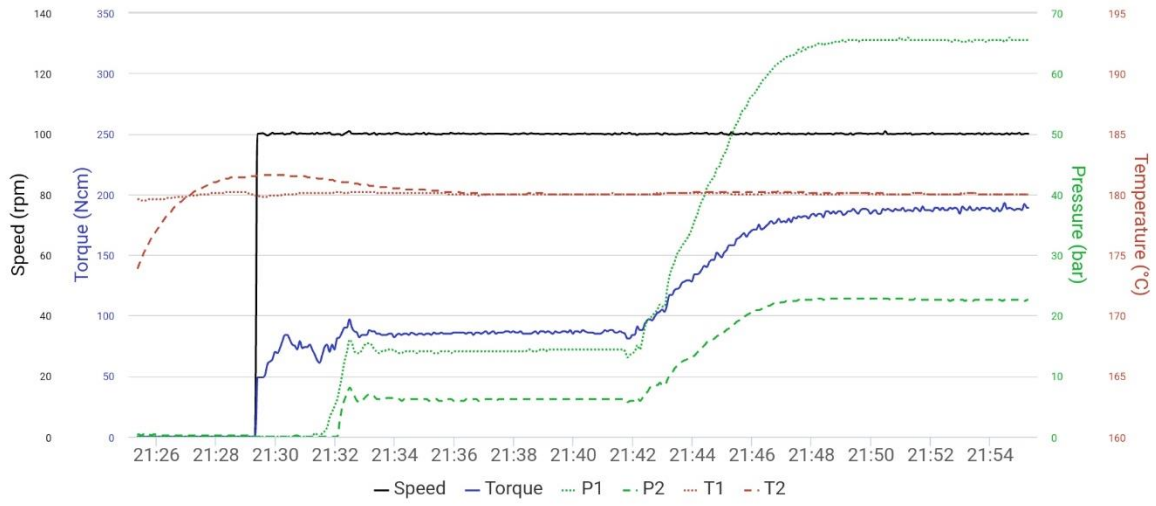

Figure S3: Evolution of torque and pressure in the twin-screw extruder during MA functionalization (initial 10 min) and subsequently during epoxy-anhydride curing process (X- axis is time scale in 24h format).

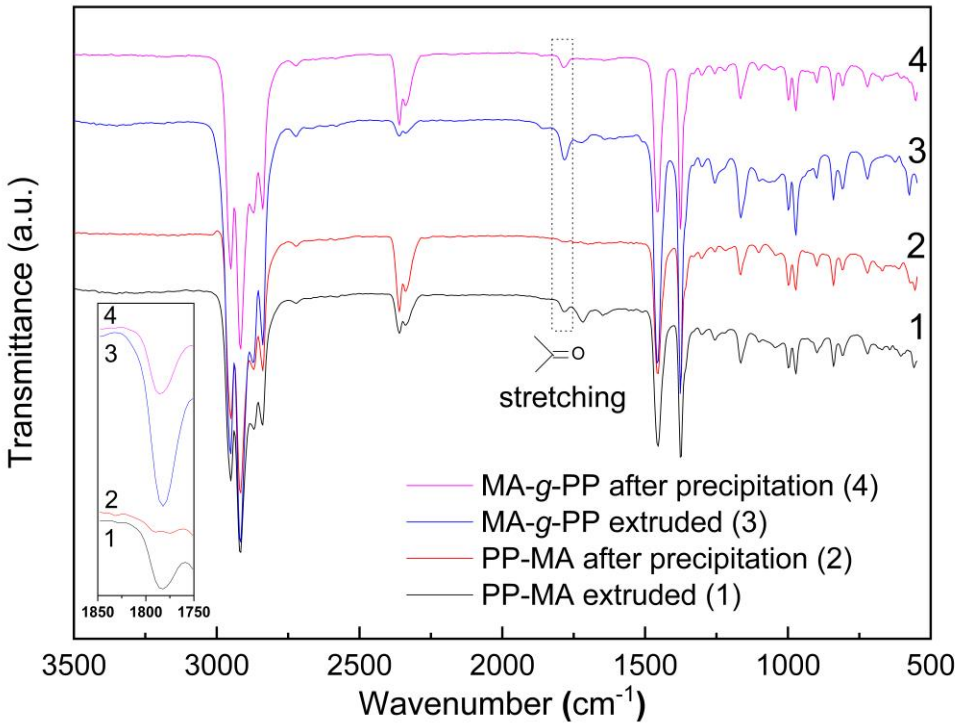

Figure S4. FT-IR spectra of different PP delineating the differences of absorbance in C=O band in the anhydride functional group. The curves 1,2 labelled PP-MA are a blend of PP with MA without initiator, so we are certain no grafting has occurred. Here, after precipitation, no anhydride peak is observed, while the MA-*g*-PP after precipitation retains the grafted anhydride (inset: showing the stretching frequency of C=O bond).

Figure S5: Insoluble fraction of PP-vitrimer (1 wt% $Zn(acac)_2$ and DGEBA/MA = 1.7) after swelling 24 hours in hot xylene (at 120 °C).

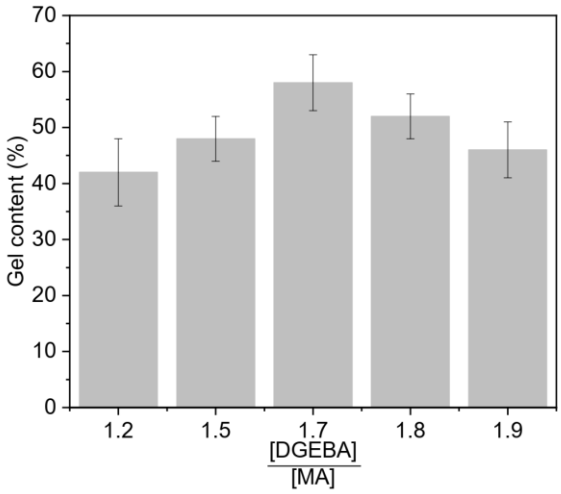

Figure S6. Extent of crosslinking by varying DGEBA content (with fixed MA content 6 wt% and 1 wt% $Zn(acac)_2$). These are very high gel fractions, comparing with other literature based on polyolefin vitrimers.

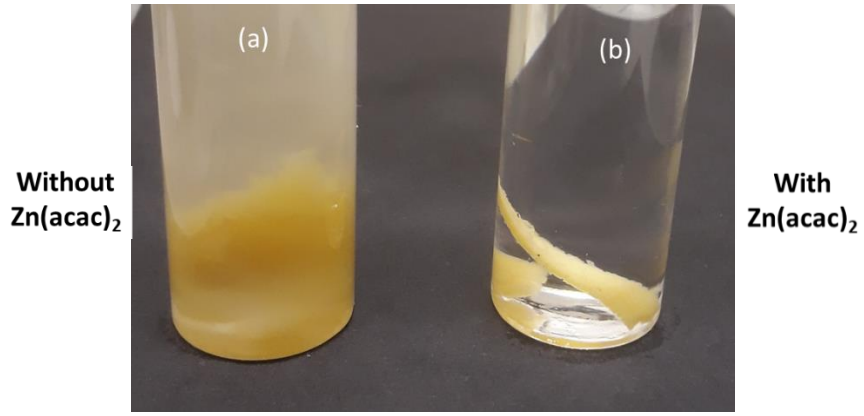

Figure S7. Swelling test for different network to show the role of catalyst. Melt extruded strand without and with catalyst, $Zn(acac)_2$ were immersed in hot xylene (at 120 °C) for 3 h. (a) The strand without catalyst (with DGEBA/MA = 1.7) start swelling in xylene and fully dispersed in solvent afterwards, (b) the strand with catalyst (1 wt% $Zn(acac)_2$ and DGEBA/MA = 1.7) does not disperse, and retains insoluble fraction (gel content = 58%).

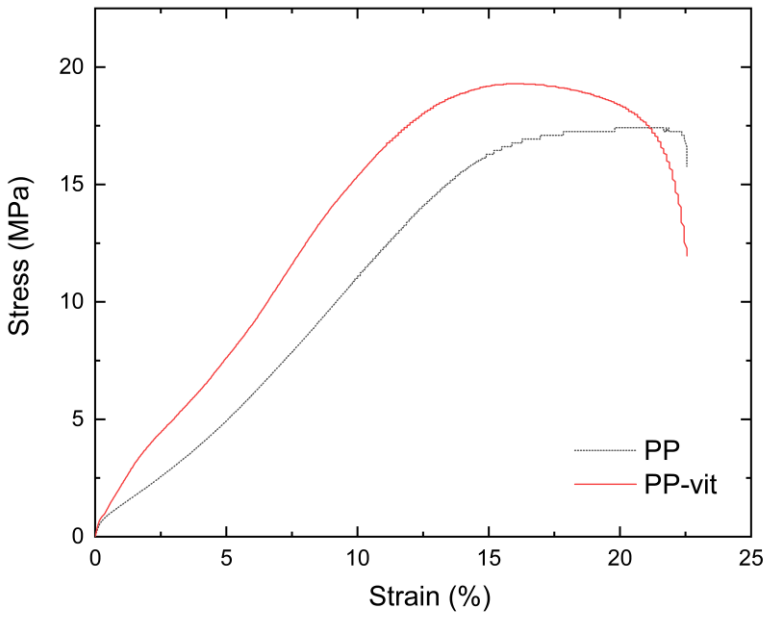

Figure S8. Tensile stress-strain response of neat PP 3950, and PP-vitrimer (with 1 wt% $Zn(acac)_2$ and DGEBA/MA = 1.7) at room temperature, with fixed crosshead speed of 10 mm/min. The crosslinking improved the tensile strength while it maintained a comparable elongation at break.

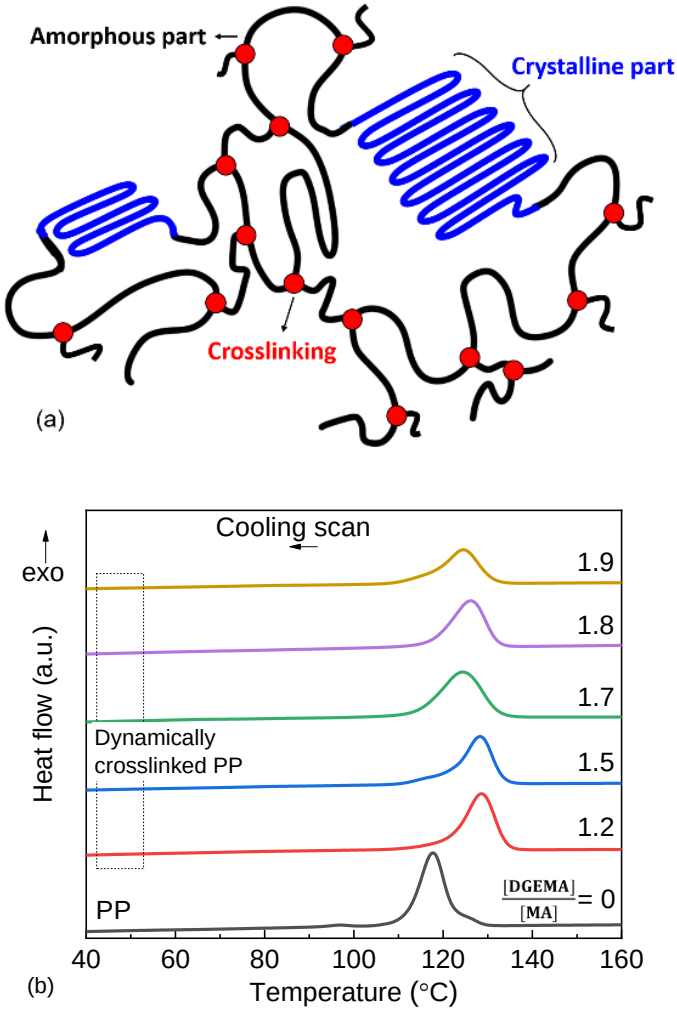

Figure S9. Network structure in semicrystalline polymer. (a) Crystallization generally occurs in the amourphous segment while the crosslinking constrains chain packing hence reducing crystallinity. (b) Exotherm from DSC cooling scan reveals crystallization temperature icreases with crosslinking, suggesting hetenucleation rendered by crosslinking microdomain.

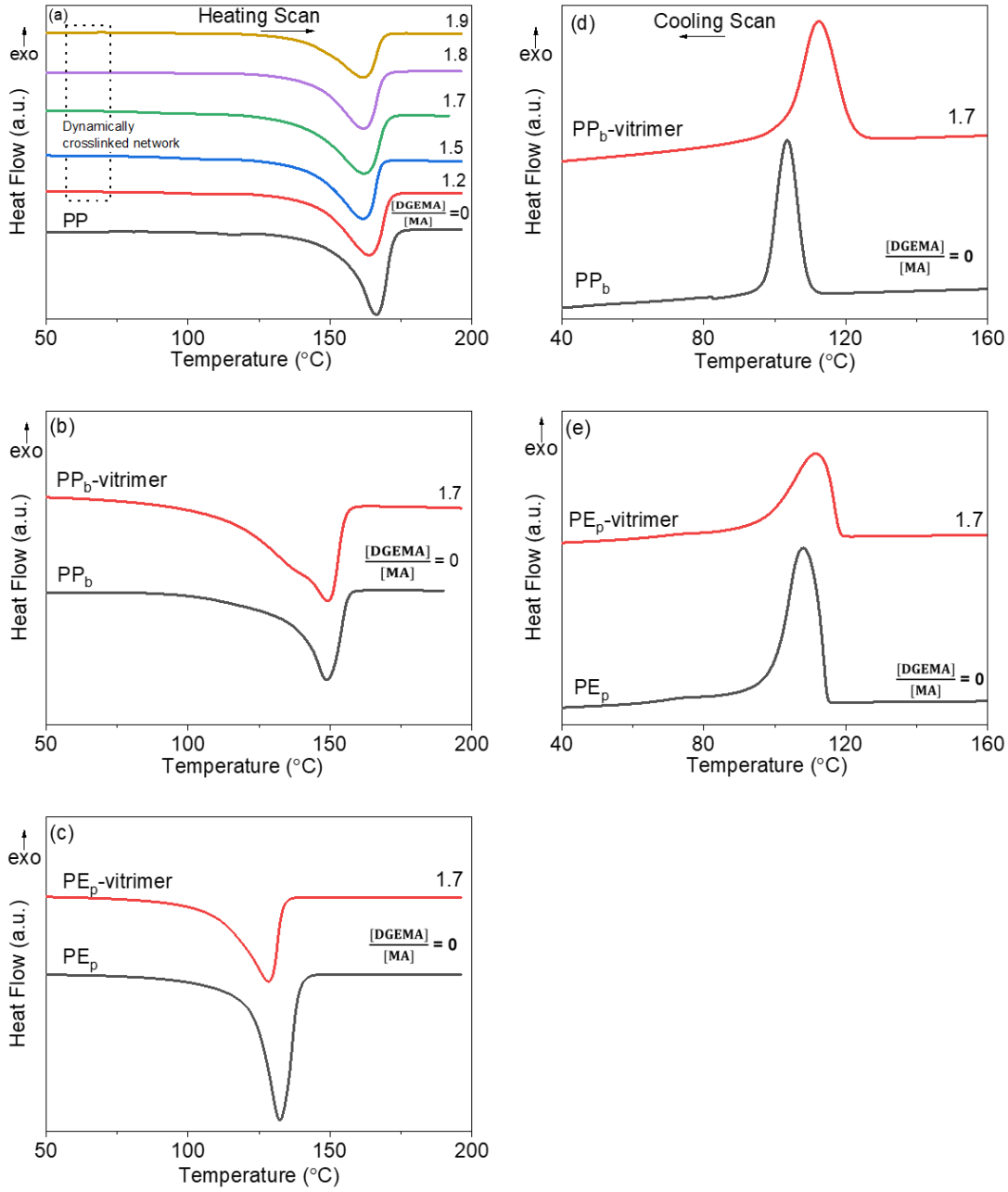

Figure S10: DSC thermogram of different crosslinked network and their precursor TPO. (a-c) DSC (2nd) heating scan showing melting endotherm, (d-e) cooling scan reveals the crystallization exotherm.

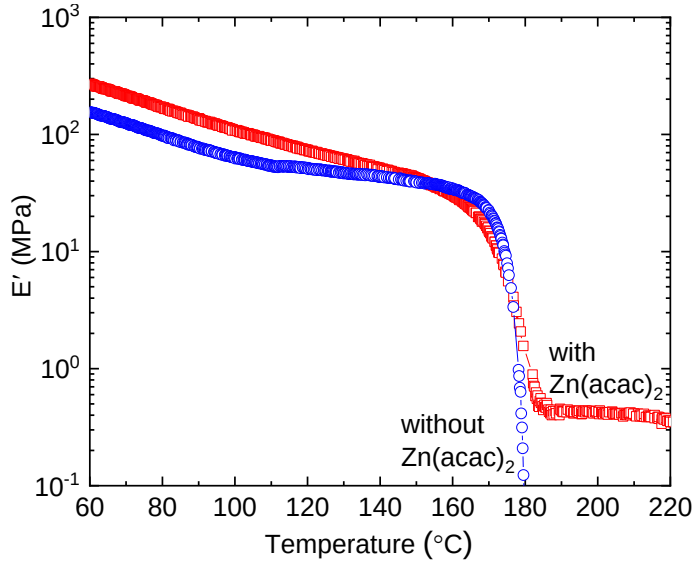

Figure S11. DMTA profile of the network (for PP) comparing the effect of catalyst $Zn(acac)_2$. Specimen without $Zn(acac)_2$ does not exhibit rubbery plateau – the signature profile for crosslinked network, in contrast to the specimen with $Zn(acac)_2$ which is PP-vit.

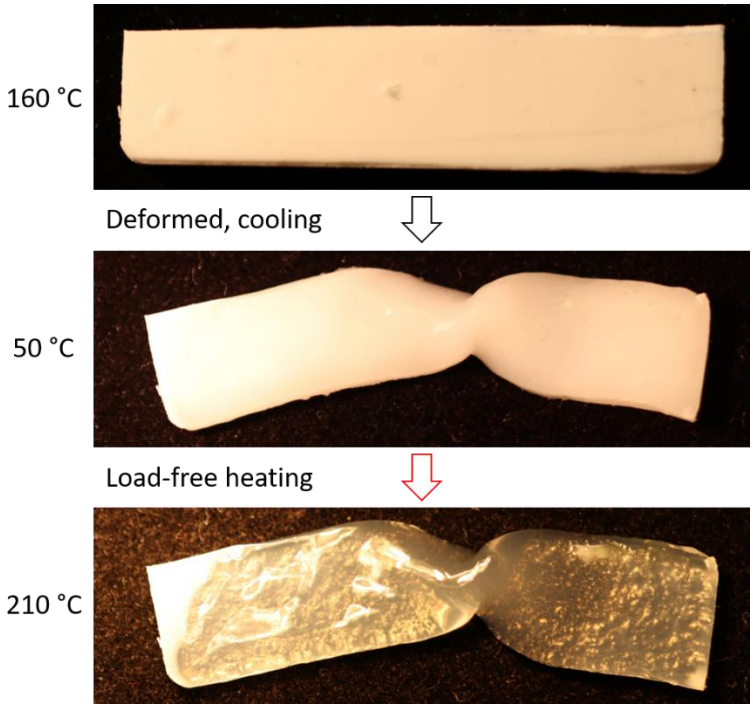

Figure S12. Neat PP was deformed at high temperature (160 °C) close to the T_m, subsequently cooled below T_c while maintained stress. This step immobilizes it to a temporal shape. The specimen was unloaded and heated to 210 °C. Thermoplastic PP does not 'remember' the original shape and flows onto the base beyond T_m. The striking difference between thermoplastic PP and PP-vit in terms of the ability to 'remember' intermediate temporal shape stems from the absence of crosslinked networks (in neat PP).

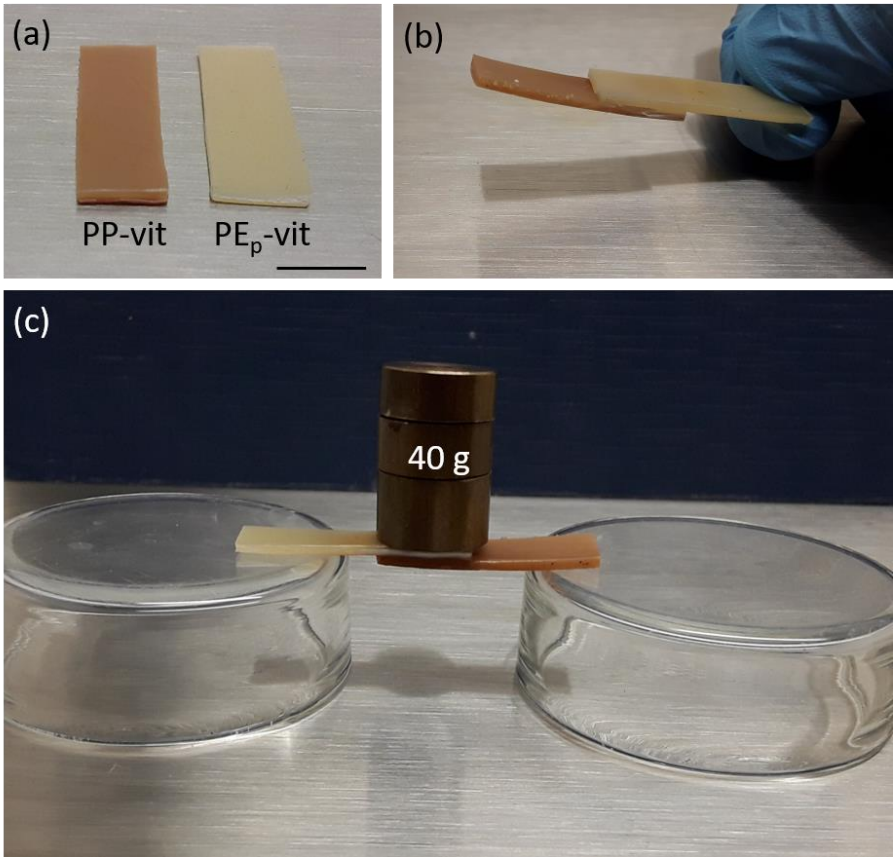

Figure S13. Welding incompatible interfaces (PP/PE). (a) Rectangular samples of PP-vit and PE_p-vit. Scale bar is 10 mm. (b) Lap joint between PE_p-vit and PP-vit. (c) Stability of joints was primarily examined placing weights for 24 h.

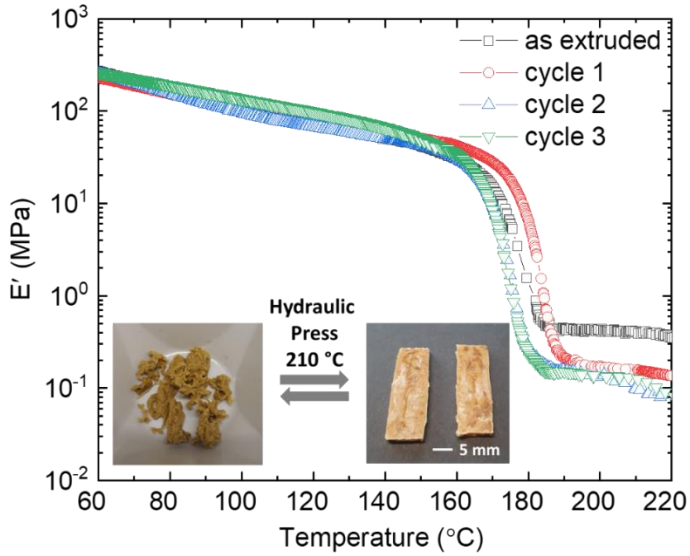

Figure S14. Topological reconfiguration through compression moulding. DMTA of reprocessed PP-vit specimen showing similar profile with slight change in rubbery regime (inset: small pieces of PP-vit are fused under hydraulic-press assuming the desired shape.).

References

1. T. Bremner, A. Rudin and D. G. Cook, *J. Appl. Polym. Sci.*, 1990, **41**, 1617-1627.
2. S. H. P. Bettini and J. A. M. Agnelli, *Polym. Test.*, 2000, **19**, 3-15.
3. M. Sclavons, P. Franquinet, V. Carlier, G. Verfaillie, I. Fallais, R. Legras, M. Laurent and F. C. Thyrion, *Polymer*, 2000, **41**, 1989-1999.
4. N. G. Gaylord and R. Mehta, *J. Polym. Sci., Part A: Polym. Chem.*, 1988, **26**, 1189-1198.
5. A. Oromiehie, H. Ebadi-Dehaghani and S. Mirbagheri, *Int. J. Chem. Eng. Appl*., 2014, **5**, 117.
6. S. Ranganathan, W. E. Baker, K. E. Russell and R. A. Whitney, *J. Polym. Sci., Part A: Polym. Chem.*, 1999, **37**, 1609-1618.
7. S. Paul, Y. Zhu, C. Romain, R. Brooks, P. K. Saini and C. K. Williams, *Chem. Commun.*, 2015, **51**, 6459-6479.
8. T. Vidil, F. Tournilhac, S. Musso, A. Robisson and L. Leibler, *Prog. Polym. Sci.*, 2016, **62**, 126-179.
9. X. Fernàndez-Francos, X. Ramis and À. Serra, *J. Polym. Sci., Part A: Polym. Chem.*, 2014, **52**, 61-75.
10. M. Giebler, C. Sperling, S. Kaiser, I. Duretek and S. Schlögl, *Polymers*, 2020, **12**, 1148.